Response to Reviewer 2

Ms. No: Preprint nhess-2023-191

Title: **Shoreline and Land Use Land Cover Changes along the 2004 tsunami-affected South Andaman Coast: Understanding Changing Hazard Susceptibility.**
https://doi.org/10.5194/nhess-2023-191

In this response file, the text in blue shows the comments from reviewers, while the black text is our replies.

We highly appreciate the learned reviewer for his keen interest in reviewing our manuscript. His insightful comments and constructive feedback have helped enhance the quality of the manuscript. We have included most of the suggestions in the revised manuscript. Hope you find them appropriate.

Reviewers comment

The author adopted the TUNAMI-N2 model to evaluate the area submerged by the tsunami flow. The authors should describe: i) the model, ii) the calibration parameters and how they are selected; and iii) the characteristics of the computational grid. The model is applied to a real event, therefore a validation with some field data could be useful.

Reply

The TUNAMI-N2 model and Computational grids

The TUNAMI-N2 model is a numerical simulation tool widely employed for modeling tsunami propagation and inundation dynamics. Specifically, it utilizes finite-difference methods to solve the shallow water wave equations, incorporating factors such as bathymetry data, earthquake source parameters, and fault geometry to simulate tsunami behavior. The TUNAMI-N2 code utilizes input data organized into three columns: X-coordinate (Longitude), Y-coordinate (Latitude), and Z-values representing elevations (negative for land elevations and positive for ocean depths). These data are initially formatted and processed using Surfer software to convert into evenly spaced grids. We adopted a grid spacing ratio of 1:3 across all four grids. Grids A and B, designed to model linear effects in deep-sea regions, were set at resolutions of 81 arc seconds and 27 arc seconds, respectively. Conversely, grids C and D, aimed at capturing the non-linear effects of the tsunami, were maintained at constant resolutions of 9 arc seconds and 3 arc seconds, respectively. As the tsunami wave propagates from deep waters to shallow waters the non-linear effects come into the picture i.e. amplitude dispersion, energy dissipation, bottom friction, and shallow depths. The program assumes non-linear theory to estimate the run-ups and impact. This program uses nesting of grids with accurate bathymetry and topography data to simulate the tsunami i.e. A, B, C, and D grids. We used coarser resolution bathymetry and topography data to model the initial deformation and propagation to save CPU time. Nested grids minimize errors by ensuring a sufficient number of nodes within each wavelength to accurately resolve the wave. In deep water, where wavelengths are longer, relatively coarse grids suffice to resolve the wave with minimal error, as fewer nodes are needed. However, as the wave propagates into shallower waters, the wavelength shortens and the amplitude increases. This necessitates finer resolution grids with more node points to accurately capture the wave dynamics and prevent errors. Therefore, higher-resolution grids are required in shallow waters to ensure an accurate representation of wave behavior. We considered the spacing of grids in such a way that it satisfies the Courant-Friedrich-Lewy conditions for checking the convergence of the numerical code to a certain asymptotic limit.

$$\Delta x/\Delta t = \sqrt{(2gh_{max})}$$

Where Δt and Δx are temporal and spatial grid sizes, hmax maximum still water depth in the computational domain, and g is the gravitational acceleration. In our study, we considered spatial grid spacing by keeping the time step constant i.e. 15 seconds, and temporal grid spacing of 1 second.

Apart from the bathymetry and topography data, one should have precise focal mechanism solutions and fault parameters to compute the initial deformation at the source at t=0 seconds. This code uses Mansinha and Smyile's (1971) deformation model to estimate the seafloor upliftment near the source. TUNAMI-N2 code allows the tsunami wave to propagate freely in the open sea and for that, we have to consider the exterior grid (A) in a very large domain as the tsunami propagates transoceanic regions and is interpolated into the B, C, and D grids. After giving the required inputs the program is compiled and executed to get the directivity map, wave amplitudes at different tide-gauge locations, and run-up heights at different locations in the study region.

Calibration Parameters and how they select:

The calibration parameters include bathymetry resolution, earthquake source parameters (e.g., slip distribution, fault length, and width), and grid resolution. These parameters were carefully selected based on established literature (e.g., Ioualalen, 2007; Rani et al., 2011; Srivastava et al., 2021) and sensitivity analyses to ensure their appropriateness for capturing the characteristics of the 2004 Sumatra earthquake and subsequent tsunami.

Validation with Field Data:

We have validated our model results with field data as shown in Figure 3 of the manuscript. We also used the observations of Cho et al. (2008) and Prerna et al. (2015) to highlight the consistency of our findings with respective field studies and we have visited several coastal locations in their study. The agreement underscores the reliability of our numerical simulations.

Regarding the shoreline changes, uncertainty must be evaluated. Due to the low slope of the beach in some transects, uncertainty must be correlated with the water level (tide and barotropic surge).

The evaluation of uncertainty encompasses various factors, including natural and anthropogenic forces such as wind, waves, tides, currents, and human influences, along with the accuracy of measurement techniques, including digitization, interpretation, and GPS error. Special attention has been given to the influence of tides on Landsat satellite imagery used in shoreline analysis. Even though, because of the large coastline extent of the study area, the tidal difference would only be visible to an inconsiderable amount.

As tide gauge data for Port Blair station is unavailable for the years 2004-2005 and 2022, we have calculated uncertainty using available data from 2018-2019 and 2019-2020 obtained from the Permanent Service for Mean Sea Level (PSMSL) database (https://psmsl.org/data/obtaining/stations/206.php). The calculated uncertainty values for these years are 7.46 meters and 7.13 meters, respectively. To quantify uncertainty, we have adopted a confidence interval of 90% and assigned a shoreline uncertainty value of 10 meters. This aligns with recommendations from the U.S. Geological Survey (USGS), which suggests a default value of 10 meters based on recent regional reports under the National Assessment of Shoreline Change project (Himmelstoss et al., 2021; Den and Oele, 2018 and Joesidawati, 2016).

We have incorporated this aspects in the revised manuscript as well.

NSM and EPR are not “statistical” parameters, since they are related to the difference between two observations.

We agree that EPR (End Point Rate) and NSM (Net Shoreline Movement) are not statistical parameters. EPR and NSM are not considered statistical parameters because they do not involve the estimation of parameters based on sample data or statistical inference. Instead, they are quantitative measures derived from observed data (i.e., shoreline positions) over specific time intervals. They represent the calculated rates of shoreline change and are not inherently statistical in nature. They are used to quantify and characterize the rates of erosion or accretion along coastlines, providing valuable information for understanding coastal dynamics and assessing coastal hazards. (Himmelstoss et al, 2021; Sam and Gurugnanam, 2022; Den and Oele, 2018; Ciritci and Türk, 2020).

However, mean values of these parameters have been computed and we mentioned them as statistical parameter primarily based on Himmelstoss et al., 2021, where it is referred as Statistical Parameter.

We have modify the text in revised manuscript to clear this ambiguity.

Minor points:

1. L. 48-50 – check the sentence.

Reply: Sentence corrected in the revised manuscript.

2. Figure 3 a and b – please add labels in the axes and the colour bars.

Reply: Labels axes is now added and the colour bar is already present in Figures 3 a and b

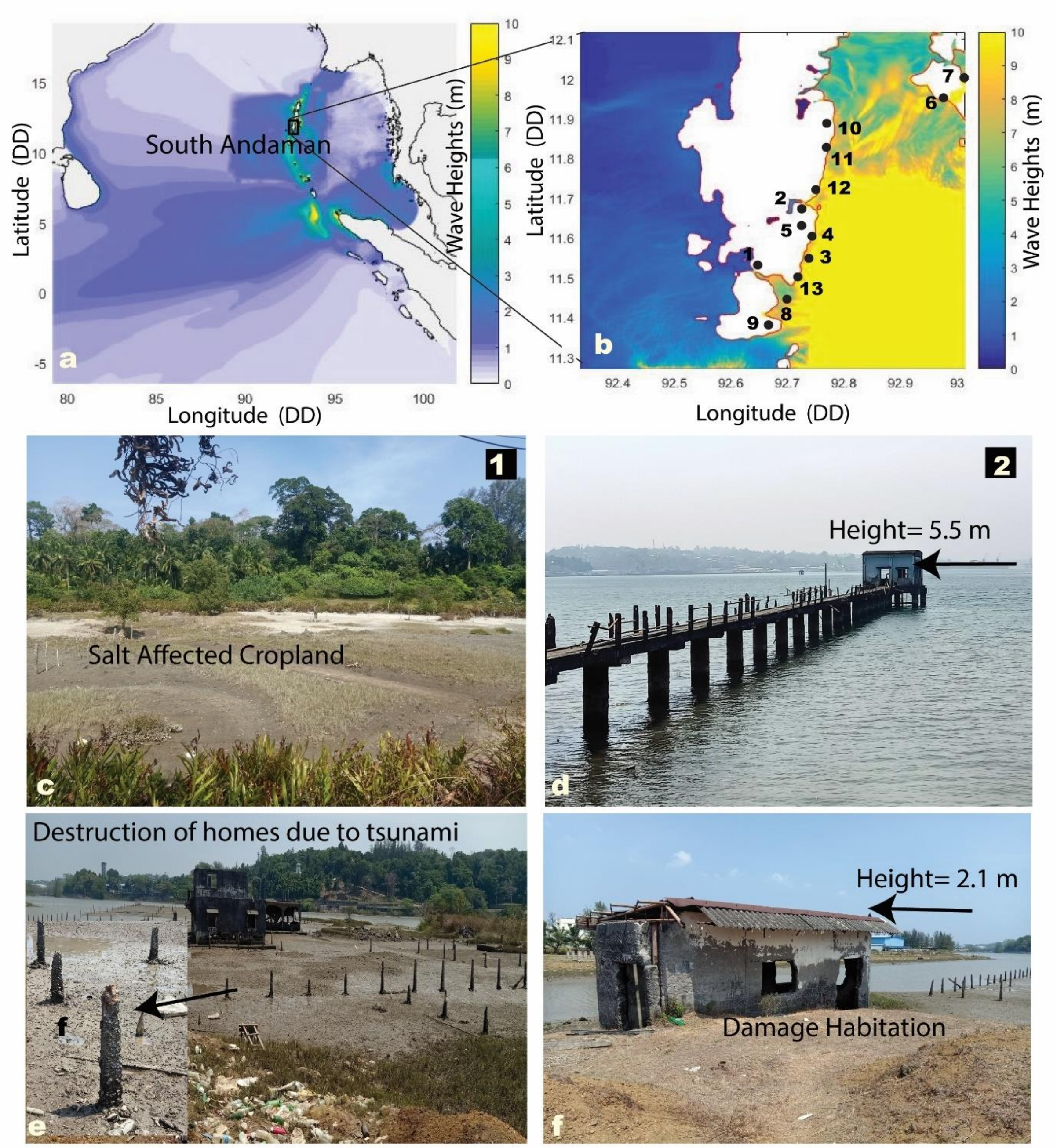

3. L, 226 – Delete "rates". EPR is already a rate.

Reply: "rate" is now deleted

4. Figure 5 – the axis labels are too small.

Reply: Axis label size is now increases

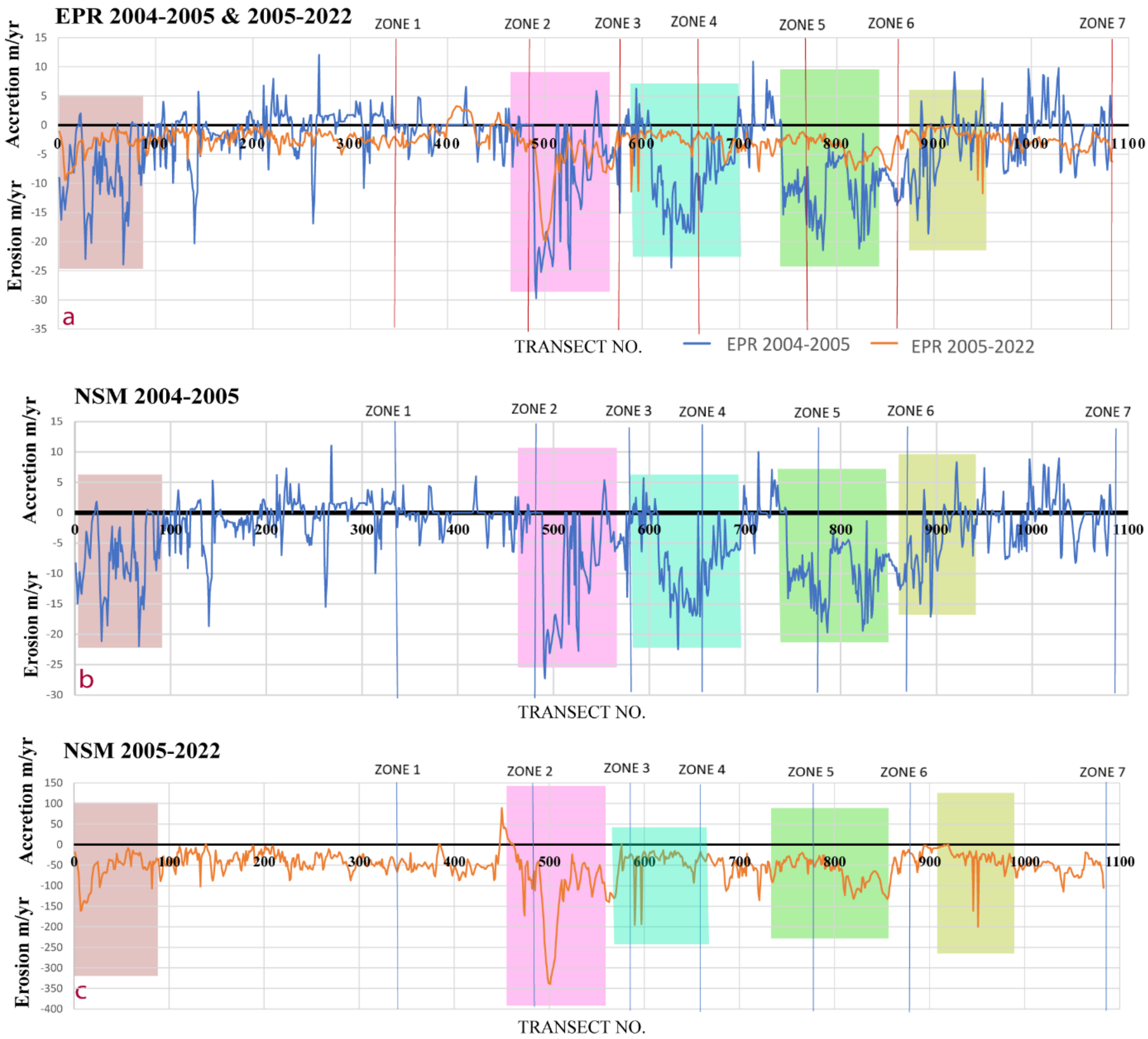

5. pages 14-15 – Check the reference to figures SM1 – SM4,

Reply: SM1 – SM7 is now changed to S1, S2…S7

6.L. 285-288. Are you sure about the change in water depth? The ground colors in the 2005 and 2022 images also show a noticeable difference.

The dark blue color in the Landsat images from 2004 and 2005 suggests clear water without detrital sediment load, while the light blue color in the 2022 image indicates a significant fresh sediment load with bright reflectance and we assume that it will have effect on reduction in water column depth.

References

Himmelstoss, E., Henderson, R. E., Kratzmann, M. G., & Farris, A. S. (2021). Digital shoreline analysis system (DSAS) version 5.1 user guide (No. 2021-1091). US Geological Survey.

Sam, S. C., & Gurugnanam, B. (2022). Coastal transgression and regression from 1980 to 2020 and shoreline forecasting for 2030 and 2040, using DSAS along the southern coastal tip of Peninsular India. Geodesy and Geodynamics, 13(6), 585-594.

Den Boer, E. L., & Oele, A. C. (2018). Determination of shoreline change along the East-Java coast, using the Digital Shoreline Analysis System. In *MATEC Web of Conferences* (Vol. 177, p. 01022). EDP Sciences.

Ciritci, D., & Türk, T. A. R. I. K. (2020). Assessment of the Kalman filter-based future shoreline prediction method. International journal of environmental science and technology, 17(8), 3801-3816.

Joesidawati, M. I. (2016). Shoreline change in Tuban district, East Java using geospatial and digital shoreline analysis system (DSAS) techniques. International Journal of Oceans and Oceanography, 10(2), 235-246.

Mansinha, L., and Smylie, D.E., 1971, The displacements fields of inclined faults, Bull. Seismol. Soci. Am., 61(5), 1433-1440.